Available online at www.sciencedirect.com
ScienceDirect
International Journal of Mass Spectrometry 255–256 (2006) 102–110
International Journal of Mass Spectrometry
www.elsevier.com/locate/ijms

Collision-induced dissociation of [4Fe-4S] cubane cluster complexes: $[Fe_4S_4Cl_{4-x}(SC_2H_5)_x]^{2-/1-}$ ($x = 0$–4)

You-Jun Fu [a,b], Julia Laskin [b], Lai-Sheng Wang [a,b,*]

[a] *Department of Physics, Washington State University, 2710 University Drive, Richland, WA 99352, USA*
[b] *Fundamental Science Directorate, Pacific Northwest National Laboratory, P.O. Box 999, MSIN K8-88, Richland, WA 99352, USA*

Received 30 September 2005; received in revised form 12 December 2005; accepted 12 December 2005
Available online 18 January 2006

Abstract

Collision-induced dissociation (CID) experiments on a series of [4Fe-4S] cluster ions, $[Fe_4S_4Cl_{4-x}(SC_2H_5)_x]^{2-/1-}$ ($x = 0$–4), revealed that their fragmentation channels change with the coordination environment. Among the three Coulomb repulsion related channels for the doubly charged species, the collision induced electron detachment channel was found to become more significant from $x = 0$ to 4 due to the decreasing electron binding energies and the magnitude of repulsion Coulomb barrier, while both the ligand detachment of Cl^- and the fission of the $[Fe_4S_4]^{2+}$ core became more and more significant with the increase of the Cl^- coordination, and eventually became the dominant channel at $x = 0$. From the parents containing the $-SC_2H_5$ ligand, neutral losses of HSC_2H_5 (62 u) and/or $HSCH{=}CH_2$ (60 u) were observed. It was proposed that inter- and intra-ligand proton transfer could happen during the CID process, resulting in hydrogen coordination to the [4Fe-4S] cluster. In the presence of O_2, $[Fe_4S_4Cl_3(SC_2H_5)]^{2-}$ and $[Fe_4S_4Cl_4]^{2-}$ can form the O_2-substituted products $[Fe_4S_4Cl_2(SC_2H_5)O_2]^-$ and $[Fe_4S_4Cl_3O_2]^-$, respectively. It was shown that the O_2 complexation occurs by coordination to the empty iron site of the [4Fe-4S] cubane core after dissociation of one Cl^- ligand.

Keywords: Mass spectrometry; Fourior transform ion cyclotron resonance; FTMS; Fe–S cluster; Fe–S protein; Collision-induced dissociation; MS/MS

1. Introduction

Iron–sulfur proteins are involved in a wide range of vital biological processes, such as respiration, photosynthesis, and nitrogen fixation [1–3]. The active sites of these proteins normally contain iron–sulfur clusters with one to four iron atoms, among which the cubane [4Fe-4S] cluster is the most prototypical [4]. We are interested in understanding the intrinsic electronic structure and chemical bonding of Fe–S clusters, which determine their functionality in Fe–S proteins. We have been able to transport a variety of synthetic Fe–S analogue complexes from solution into the gas phase using electrospray ionization (ESI) and systematically investigated their electronic properties using photoelectron spectroscopy (PES) [5–8]. In combination with broken symmetry density functional calculations, our studies on the doubly charged cubane-type anions, $[Fe_4S_4L_4]^{2-}$, have confirmed the "inverted energy scheme" of their electronic structure [5,6]. The PES data provided the intrinsic oxidation potentials of the complexes, revealing their dependence on the terminal ligands and the electrostatic nature of the interactions between the cubane core and the terminal ligands. During these studies, we have also observed unexpectedly symmetric fissions of the doubly charged cubane complexes, $[Fe_4S_4L_4]^{2-} \rightarrow 2[Fe_2S_2L_2]^-$, through collision-induced dissociation (CID) [9–11], which provides direct experimental evidence for the two-layer spin-coupling model for the [4Fe-4S] cubane core [12–14]. Similar symmetric fission channels have also been observed for several mixed ligand clusters $[Fe_4S_4L_xL'_{4-x}]^{2-}$ [15]. In our most recent work using potentially bidentate ligands, we observed ligand reorganizations following fission to create novel [2Fe-2S] structures, in which the two iron sites have different coordination geometries [16]. Our PES data further showed that tetra-coordination tends to decrease the oxidization energy in the [2Fe-2S] complexes relative to tri-coordination. Using CID, we have also produced cubane clusters with various oxidation states from $[4Fe\text{-}4S]^-$ to $[4Fe\text{-}4S]^{3+}$ by losing variable terminal ligands $[Fe_4S_4L_x]^-$ [17].

In the current work, we present a detailed study of the fragmentation behavior of the [4Fe-4S] cubane clus-

* Corresponding author. Tel.: +1 509 376 5050; fax: +1 509 376 6066.
E-mail address: ls.wang@pnl.gov (L.-S. Wang).

1387-3806/$ – see front matter © 2005 Elsevier B.V. All rights reserved.
doi:10.1016/j.ijms.2005.12.009

ter complexes with mixed Cl and SEt (Et = C_2H_5) ligands, $[Fe_4S_4Cl_{4-x}(SEt)_x]^{2-}$ (x = 0–4), using a 6-Tesla FTICR mass spectrometer with an ESI source [18].

2. Experimental

All sample preparations were carried out in a dry N_2 glove box. Stock solutions of anions $[Fe_4S_4Cl_4]^{2-}$ and $[Fe_4S_4(SEt)_4]^{2-}$ were prepared by dissolving solid samples of $(t\text{-}Bu_4N)_2[Fe_4S_4Cl_4]$ and $(t\text{-}Bu_4N)_2[Fe_4S_4(SEt)_4]$ in O_2-free acetonitrile (1×10^{-4} mol/L), respectively. Mixed ligand complexes, $[Fe_4S_4Cl_{4-x}(SEt)_x]^{2-}$ (x = 1–3), were produced by electrospraying a mixed solution of the two stock solutions [5,6].

The experiments were performed on a 6 Tesla FTICR instrument at the Pacific Northwest National Laboratory [18]. Ions were generated in a high-transmission external ESI source equipped with an electrodynamic ion funnel, a collision quadruple, a mass resolving quadruple, and an accumulation quadruple. The collision quadruple was operated in RF only mode for ion collisional focusing. All ions were transmitted into and stored in the accumulation quadruple with the resolving quadruple operated in the RF only mode. The ions extracted from the accumulation quadruple were transferred into the ICR cell by a series of ion transfer lenses and captured using gated trapping.

The CID experiments were carried out in the ICR cell. A normal mass spectrum was taken to select the isotopic peak of interest (Fig. 1a). For MS/MS experiments, all unwanted ions were ejected by applying a Stored Waveform Inverse Fourier Transform (SWIFT) excitation (Fig. 1b) [19,20]. SORI (sustained off-resonance irradiation)-CID experiments [21] were performed on single isotopic peaks. Ar was utilized as a collision gas, which was introduced into the cell using a pulsed valve.[1] The isolated precursor ions were radially excited slightly off resonance for 40 ms with collision energies optimized in the range of 0.5–1.7 eV by changing the peak-to-peak voltage applied to the excitation plates. After 10 s pumping delay ions in the cell were excited for detection by broadband chirp excitation (Fig. 1c and d).

Fig. 1 represents the typical experimental procedure using $[Fe_4S_4(SEt)_4]^{2-}$ as an example. Usually the most abundant isotopes were selected for CID experiments. However, for doubly charged parents, in several cases low-abundance isotopes were selected to eliminate overlap between the parent ions and their fission products. For example, since the leading isotope of $[Fe_4S_4(SEt)_4]^{2-}$ at m/z 297.8 cannot be distinguished from the leading isotope of its fission product $[Fe_2S_2(SEt)_2]^{-}$ (Fig. 1a),

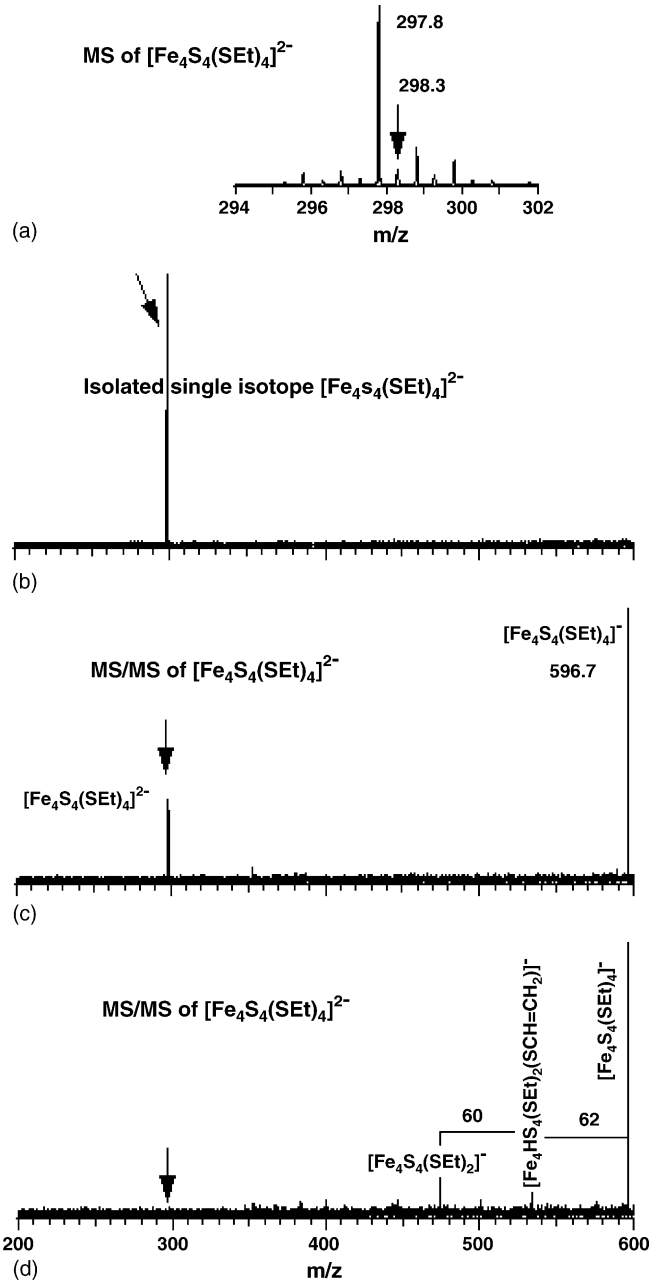

Fig. 1. Procedure of the SORI-CID experiment: (a) mass spectrum of $[Fe_4S_4(SEt)_4]^{2-}$; (b) single isotope isolation using SWIFT technique; (c) CID mass spectrum of $[Fe_4S_4(SEt)_4]^{2-}$ at a low collision energy (E_{CM} = 0.48 eV); (d) CID mass spectrum of $[Fe_4S_4(SEt)_4]^{2-}$ at a higher collision energy (E_{CM} = 0.75 eV).

SORI-CID was performed using the minor isotope at m/z 298.3 as the precursor ion, which allows us to distinguish the parent ion from its fission products in MS/MS spectra. On the other hand, the leading isotopic peak of $[Fe_4S_4Cl_4]^{2-}$ is at m/z 246.8, while the major isotope of its fission product is located at m/z 245.8 and does not overlap with the precursor ion except for the small interference from a minor isotope at m/z 246.8 with a relative abundance of only 5.6%. Thus, the leading peak at m/z 246.8 was selected as the precursor ion for SORI-CID experiments of $[Fe_4S_4Cl_4]^{2-}$ (Fig. 2a).

[1] The presence of O_2-substituted species in CID experiments that utilize Ar as a collision is puzzling. Clearly, these ions are produced from their mass-selected unmodified precursors inside the ICR cell. The O_2-substituted species produced in the ion source and transmitted into the ICR cell are efficiently ejected from the cell prior to CID during SWIFT isolation of the precursor ion. According to our SID experiments these ions are not formed during ion activation without the collision gas. We believe that formation of the O_2-substituted species in CID experiments results from O_2 contamination of the collision gas, most probably because of a small leak in the gas handling system.

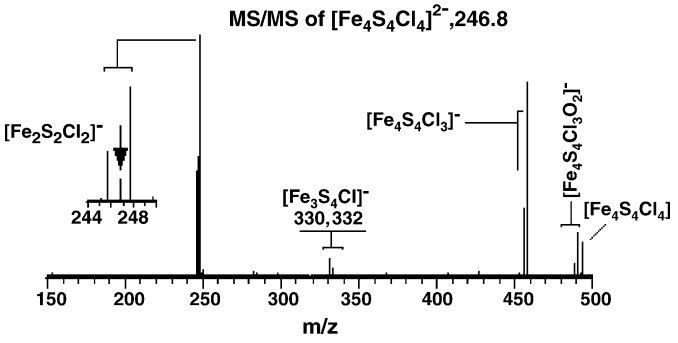

Fig. 2. CID mass spectrum of $[Fe_4S_4Cl_4]^{2-}$ ($m/z = 246.8$). See Table 1 for fragment identification. $E_{CM} = 1.75$ eV.

The maximum kinetic energy (peak–peak) achieved by off-resonance CID is given by:

$$E_{lab} = \frac{\beta^2 q^2 {V_{p-p}}^2}{8md^2\Delta\omega^2} \quad (1)$$

where m and q are the mass and the charge of the ion, respectively; $\Delta\omega = \omega - \omega_c$, with ω_c being the cyclotron frequency of the ion, and to the frequency of the excitation field; V_{p-p} is the peak-to-peak excitation voltage; β (=0.9) is the geometry factor of the cell; d is the diameter of the cell. The center-of-mass collision energy E_{CM} was calculated from E_{lab}:

$$E_{CM} = \frac{M}{M+m} E_{lab} \quad (2)$$

where M is the mass of the neutral molecule. The calculated E_{CM} represents the maximum collision energy. The real collision energy in each collision falls in the range 0–E_{CM}.

For each parent, several different collision energies were applied to take CID mass spectra. The typical results are shown in Figs. 1–9. The major fragmentation channels for $Fe_4S_4Cl_{4-x}(SEt)_x]^{2-}$ ($x = 0$–4) are summarized in Table 1 and the fragments from singly charged species are listed in the respective figure captions.

For surface-induced dissociation (SID) experiments, the resolving quadruple was operated in its mass-resolving mode

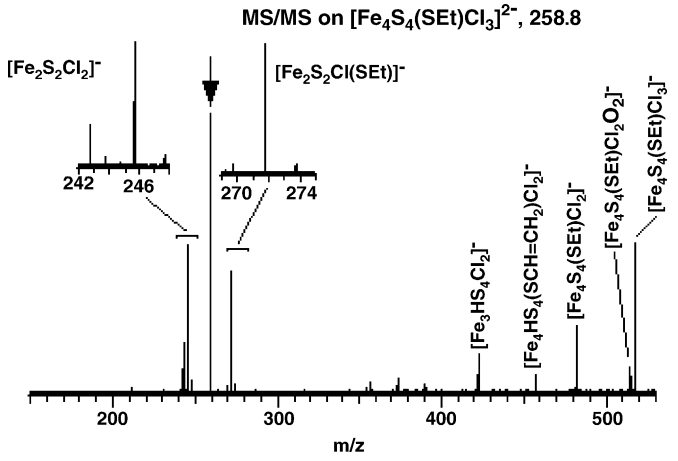

Fig. 3. CID mass spectrum of $[Fe_4S_4(SEt)Cl_3]^{2-}$ ($m/z = 258.8$). See Table 1 for fragment identification. $E_{CM} = 0.72$ eV.

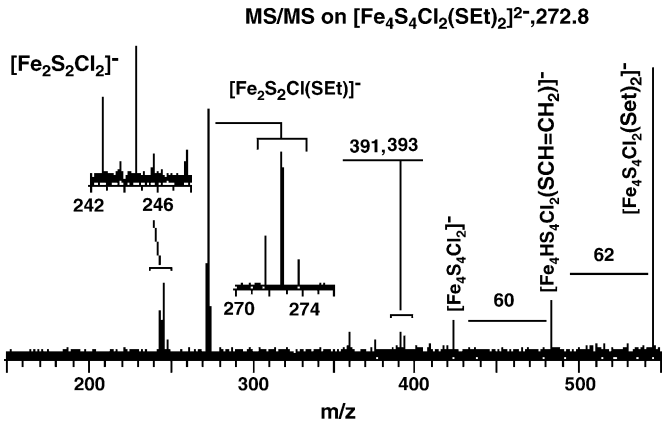

Fig. 4. CID mass spectrum of $[Fe_4S_4(SEt)_2Cl_2]^{2-}$ ($m/z = 272.8$). See Table 1 for fragment identification. $E_{CM} = 0.81$ eV.

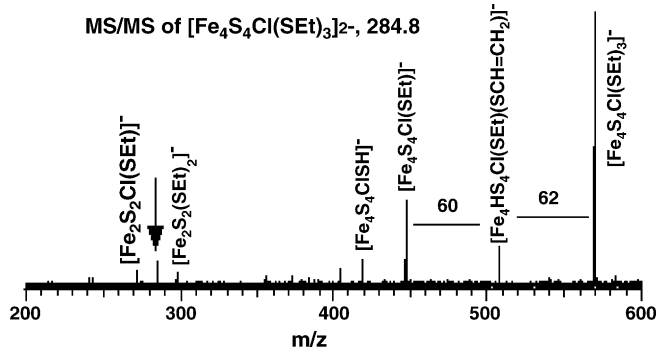

Fig. 5. CID mass spectrum of $[Fe_4S_4(SEt)_3Cl]^{2-}$ ($m/z = 284.8$). See Table 1 for fragment identification. $E_{CM} = 0.89$ eV.

with a typical dc offset in the range of 5–10 V. The isotopic envelope of the precursor ion was selected in the resolving quadruple and extracted into the electrostatic ion guide following the accumulation step. Ions were transferred through the ICR cell and

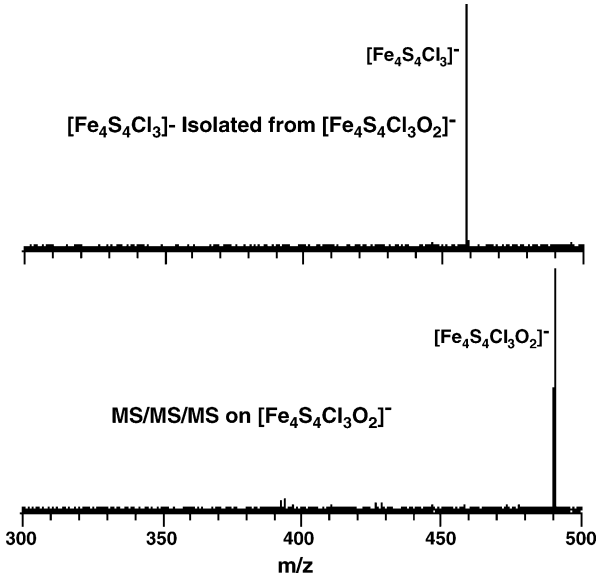

Fig. 6. MS/MS/MS spectra of $[Fe_4S_4Cl_3O_2]^-$ (a) isolated $[Fe_4S_4Cl_3]^-$ ($m/z = 458.6$); (b) attachment of O_2, $[Fe_4S_4Cl_3O_2]^-$ ($m/z = 490.5$).

Table 1
Major fragmentation channels of $[Fe_4S_4(Cl_{4-x}(SEt)_x]^{2-}$ (x = 0–4)

Parent	$[Fe_4S_4Cl_4]^{2-}$ 246.8 (18)	$[Fe_4S_4(SEt)Cl_3]^{2-}$ 258.8(100)	$[Fe_4S_4(SEt)_2Cl_2]^{2-}$ 272.8 (85)	$[Fe_4S_4(SEt)_3Cl]^{2-}$ 284.8(10)	$[Fe_4S_4(SEt)_4]^{2-}$ 298.3(10)
Fission	$[Fe_2S_2Cl_2]^-$ 247.8 (100)	$[Fe_2S_2Cl_2]^-$ 245.8 (53) $[Fe_2S_2(SEt)Cl]^-$ 271.8(43)	$[Fe_2S_2Cl_2]^-$ 244.8 (26) $[Fe_2S_2(SEt)Cl]^-$ 272.8 (86)	$[Fe_2S_2(SEt)Cl]^-$ 271.8(13) $[Fe_2S_2(SEt)_2]^-$ 297.8 (5)	
e^- loss	$[Fe_4S_4Cl_4]^-$ 493.5 (14)	$[Fe_4S_4(SEt)Cl_3]^-$ 517.6(54)	$[Fe_4S_4(SEt)_2Cl_2]^-$ 545.6(100)	$[Fe_4S_4(SEt)_3Cl]^-$ 569.6(100)	$[Fe_4S_4(SEt)_4]^-$ 596.7 (100)
Cl^- loss	$[Fe_4S_4Cl_3]^-$ 458.6 (80)	$[Fe_4S_4(SEt)Cl_2]^-$ 482.6 (24)			
O_2 attachment	$[Fe_4S_4Cl_3O_2]^-$ 490.5 (18)	$[Fe_4S_4(SEt)Cl_2O_2]^-$ 514.6(9)			
Loss of 62 CH_3CH_2SH			$[Fe_4HS_4LCl_2]^-$ 483.6 (20)	$[Fe_4HS_4(SEt)LCl]^-$ 507.6(15)	$[Fe_4HS_4(SEt)_2L]^-$ 534.7 (9)
Loss of 60 CH_2=CHSH		$[Fe_4HS_4Cl_3]^-$ 457.6 (7)	$[Fe_4S_4Cl_2]^-$ 423.6(13)	$[Fe_4S_4(SEt)Cl]^-$ 447.6 (10)	$[Fe_4S_4(SEt)_2]^-$ 474.7 (14)

SEt: $-SC_2H_5$; L: CH_2=CHS; the number under each formula is the m/z value and the relative abundance is in the bracket.

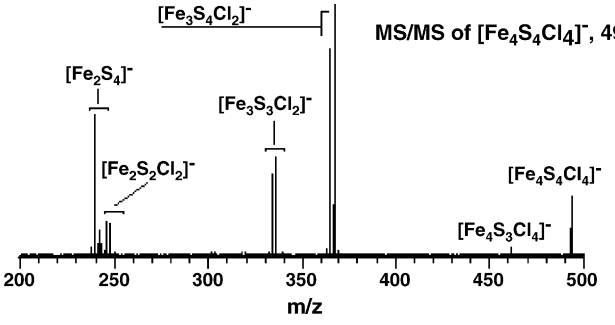

Fig. 7. CID mass spectrum of $[Fe_4S_4Cl_4]^-$ (m/z = 493.5). Fragments: $[Fe_4S_3Cl_4]^-$ (m/z = 461.5); $[Fe_3S_4Cl_2]^-$ (m/z = 367.6); $[Fe_3S_3Cl_2]^-$ (m/z = 335.7); $[Fe_2S_2Cl_2]^-$ (m/z = 245.8); $[Fe_2S_4]^-$ (m/z = 239.8). E_{CM} = 1.39 eV.

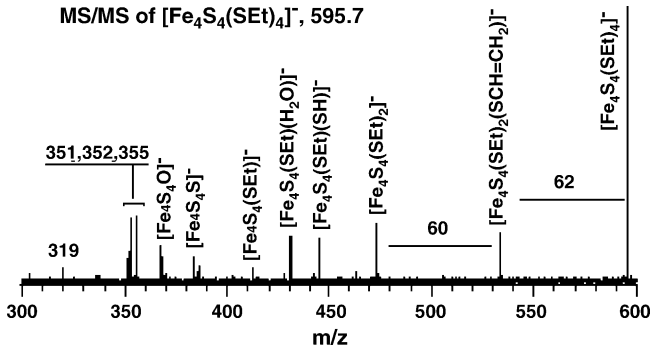

Fig. 8. CID mass spectrum of $[Fe_4S_4(SEt)_4]^-$ (m/z = 595.7). Fragments: $[Fe_4HS_4(SEt)_2\ (SCH{=}CH_2)]^-$ (m/z = 533.7); $[Fe_4S_4(SEt)_2]^-$ (m/z = 473.7); $[Fe_4S_4(SEt)S]^-$ (m/z = 445.7); $[Fe_4S_4(SEt)]^-$ (m/z = 412.7); $[Fe_4S_4S]^-$ (m/z = 383.6); $[Fe_4S_4(SEt)H_2O]^-$ (m/z = 430.6); $[Fe_4S_4O]^-$ (m/z = 367.6). E_{CM} = 0.59 eV.

collided with a fluorinated self-assembled monolayer (FSAM) surface at normal incidence [18,23–25].

3. Results and discussion

SORI-CID is a low-collision energy process. With each collision adding only a small amount of energy to the ion, the energy

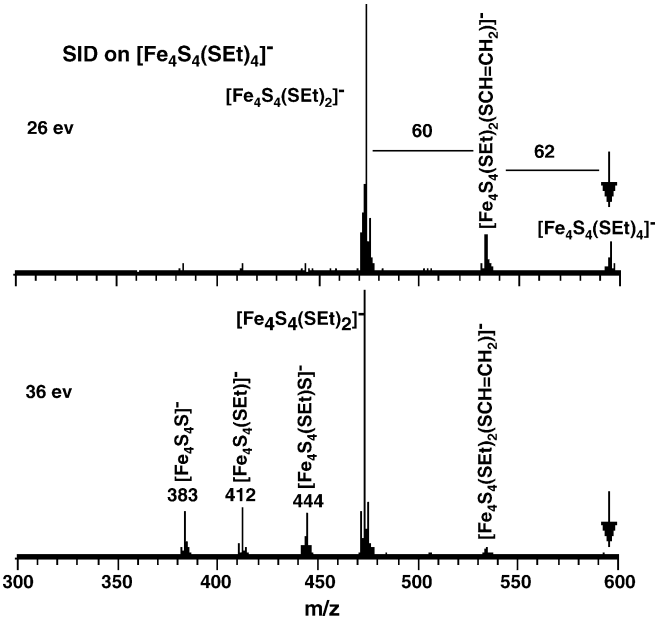

Fig. 9. SID on $[Fe_4S_4(SEt)_4]^-$ (m/z = 595.7) at different collision energy: (a) 26 eV (b) 36 eV. Fragments: $[Fe_4S_4(SEt)_2]^-$ (m/z = 473.7); $[Fe_4S_4(SEt)S]^-$ (m/z = 444.7); $[Fe_4S_4(SEt)]^-$ (m/z = 412.7); $[Fe_4S_4S]^-$ (m/z = 383.6).

is randomized throughout the molecule and multi-collision event is needed to accumulate enough internal energy to induce fragmentation. In this process, only ions with cyclotron frequencies near the applied RF frequency are excited, while the fragments, with cyclotron frequencies no longer in near-resonance with the RF signal, not further accelerated by the excitation field, will cool off and stabilize. This explains the ability of SORI-CID to access the low-energy fragmentation channels.

Figs. 1–5 show MS/MS spectra of the doubly charged parents. We noted that all the fragments are singly charged species reflecting the great tendency for the two charges of the dianions to be separated due to Coulomb repulsion, either by losing one electron or by being split into two parts. Singly charged fragment ions can undergo further fragmentation to give neutral losses and smaller fragments.

3.1. Intramolecular Coulomb repulsion and fragmentation of the doubly charged [4Fe-4S] clusters

As shown previously [26–28], doubly charged anions in the gas phase exhibit unique properties due to the presence of strong intra-molecular Coulomb repulsion derived from the excess charges. Doubly charged [4Fe-4S] cubane complexes show characteristics of intramolecular Coulomb repulsion in their fragmentation behavior. From the MS/MS spectra of $[Fe_4S_4Cl_{4-x}(SEt)_x]^{2-}$ (x = 0–4) (Figs. 1–5), three fragmentation channels related to Coulomb repulsion are observed: (1) collision-induced electron detachment; (2) collision-induced loss of charged ligand, Cl^-; and (3) collision-induced fission of the cubane core.

3.1.1. Collision-induced electron detachment

As shown in Figs. 1–5, all MS/MS spectra of the doubly charged parents $[Fe_4S_4Cl_{4-x}(SEt)_x]^{2-}$ (x = 0–4) displayed collision-induced electron detachment to give the corresponding singly charged species, $[Fe_4S_4Cl_{4-x}(SEt)_x]^-$ formulated as,

$$[Fe_4S_4Cl_{4-x}(SEt)_x]^{2-} \rightarrow [Fe_4S_4Cl_{4-x}(SEt)_x]^- + e^- \quad (3)$$

The propensity of this channel increases with x and becomes the dominant channel for x = 3 (Fig. 5) and 4 (Fig. 1c,d). This observation is consistent with the electron binding energies of these complexes [6]. Because of the strong intramolecular coulomb repulsion the $[Fe_4S_4(SEt)_4]^{2-}$ complex possesses a very low electron binding energy of 0.29 eV [5]. We have previously demonstrated that because of the strong electron withdrawing capability of the Cl ligand, electron binding energies of the Cl^- substituted $[Fe_4S_4Cl_{4-x}(SEt)_x]^{2-}$ complexes increase systematically with the Cl^- content to 0.41, 0.52, 0.62, and 0.80 eV, respectively, with x deceasing from 3 to 0 [5,6]. Despite the presence of the repulsive coulomb barrier (RCB) against electron detachment from multiply charged anions, the low electron binding energy of $[Fe_4S_4(SEt)_4]^{2-}$ makes it extremely facile for electron detachment upon collision mainly by electron tunneling through the RCB. Fig. 1c shows that at low collision energies the electron detachment channel is exclusive for $[Fe_4S_4(SEt)_4]^{2-}$ (298.3) to produce $[Fe_4S_4(SEt)_4]^-$ (596.7). Only at a higher collision energy two minor peaks appeared at m/z 474.7 and 534.7 (Fig. 1d) due to further fragmentation of the singly charged $[Fe_4S_4(SEt)_4]^-$ as will be discussed below.

3.1.2. Collisional loss of Cl^-

This CID channel was only observed for $[Fe_4S_4Cl_4]^{2-}$ (246.8) (Fig. 2) and $[Fe_4S_4Cl_3(SEt)]^{2-}$ (259.8) (Fig. 3), as shown by the prominent $[Fe_4S_4Cl_3]^-$ (458.6) and $[Fe_4S_4Cl_2(SEt)]^{1-}$ (482.6) peaks, respectively, together with the observation of Cl^- (35.0) at the low mass range (not shown). This CID channel also results from the intramolecular Coulomb repulsion because two negatively charged daughter ions are produced:

$$[Fe_4S_4Cl_4]^{2-} \rightarrow [Fe_4S_4Cl_3]^{1-} + Cl^- \quad (4)$$

$$[Fe_4S_4Cl_3(SEt)]^{2-} \rightarrow [Fe_4S_4Cl_2(SEt)]^{1-} + Cl^- \quad (5)$$

Interestingly, this channel only becomes prominent for the parent dianions, for which the collisional electron loss channel is relatively weak, whereas it is not observed for $[Fe_4S_4Cl(SEt)_3]^{2-}$ and $[Fe_4S_4Cl_2(SEt)_2]^{2-}$, for which the electron loss channel is dominant. We did not observe collisional loss of a negatively charged EtS^- ligand (m/z = 61) for any parent cubane complexes. One reason is the dominance of the electron loss channel for $[Fe_4S_4(SEt)_4]^{2-}$ and $[Fe_4S_4Cl(SEt)_3]^{2-}$, and another reason is probably the strong Fe–S covalent bonding, which makes the –SEt loss less competitive relative to the Cl^- loss when they coexist in $[Fe_4S_4Cl_2(SEt)_2]^{2-}$ and $[Fe_4S_4Cl_3(SEt)]^{2-}$.

3.1.3. Collision-induced fission of the [4Fe-4S] core

The most dramatic effect of the intramolecular coulomb repulsion in the doubly charged cubane complexes is collision-induced fission of the [4Fe-4S] core, first observed in $[Fe_4S_4X_4]^{2-}$ (X = Cl, Br, SEt) [9,10]. This process may have important implications in understanding cluster transformations in Fe–S proteins and detailed fission mechanisms have been investigated recently using density functional calculations [11]. Here, for the mixed ligand systems with x = 1–3, we observed similar fission processes despite the asymmetric coordination environments:

$$[Fe_4S_4Cl_3(SEt)]^{2-} \rightarrow [Fe_2S_2Cl_2]^{1-} + [Fe_2S_2Cl(SEt)]^{1-} \quad (6)$$

$$[Fe_4S_4Cl_2(SEt)_2]^{2-} \rightarrow 2[Fe_2S_2Cl(SEt)]^{1-} \text{ or } [Fe_2S_2Cl_2]^{1-} + [Fe_2S_2(SEt)_2]^{1-} \quad (7)$$

$$[Fe_4S_4Cl(SEt)_3]^{2-} \rightarrow [Fe_2S_2(SEt)_2]^{1-} + [Fe_2S_2Cl(SEt)]^{1-} \quad (8)$$

Our previous observation of the symmetric fission in $[Fe_4S_4X_4]^{2-}$ complexes provided direct evidence for the two-layer spin-coupling model of the cubane core [9]. The current observation indicated that the asymmetric terminal ligand coordination does not alter the two-layer electronic structure of the cubane. It is interesting to note that for $[Fe_4S_4Cl_2(SEt)_2]^{2-}$ and $[Fe_4S_4Cl(SEt)_3]^{2-}$, where no Cl^- loss was observed (Figs. 4 and 5), the fission channel still persisted. It is surprising that the fission process, which requires breaking four Fe–S bonds is even more facile than breaking of a single Fe–Cl bond. The propensity of fission seems to increase with increase of Cl content in $[Fe_4S_4Cl_{4-x}(SEt)_x]^{2-}$. This trend, similar to that of the Cl^- loss, appears to be the opposite of the electron loss channel. For $[Fe_4S_4Cl_4]^{2-}$, for which the electron loss channel is relatively minor, the fission channel is dominant, whereas for $[Fe_4S_4(SEt)_4]^{2-}$, for which the electron loss channel is dominant, fission is minor. In fact, Fig. 1 did not show any observable fission at all for $[Fe_4S_4(SEt)_4]^{2-}$, which require a much higher collision energy [9,10]. In our previous CID study using a LCQ mass spectrometer, we used a much higher collision energy and observed the fission channel from this species. SORI CID exper-

iments reported here used much lower collision energy so only fragmentation channel with relatively low reaction barriers were observed.

3.2. Dioxygen coordination of the [4Fe-4S] cluster

The formation of $[Fe_4S_4Cl_3O_2]^-$ was first observed in our previously reported CID experiments of $[Fe_4S_4X_4]^{2-}$ (X = Cl, Br, I) carried out using an LCQ mass spectrometer [10]. N_2 was used as the collision gas in that experiment. In the current work we used Ar as the collision gas showing also explicitly the O_2 substitution species.[1] With careful calibration, $[Fe_4S_4Cl_3O_2]^-$ was further identified by its exact *m/z* value 490.5449 (calc. 490.5431) and its *m/z* difference of 31.9932 from $[Fe_4S_4Cl_3]^-$, 458.5517 (calc. 458.5533) corresponding to the O_2 addition. As reported in the earlier paper $[Fe_4S_4Cl_3O_2]^-$ could be easily produced in the source. To make further identification, its isotope at 490.5 was isolated in the cell and SORI CID was carried out (Fig. 6). The spectrum showed a major peak at 458.5 identified as $[Fe_4S_4Cl_3]^-$, i.e., O_2 detachment occurred. MS/MS/MS were carried out on $[Fe_4S_4Cl_3]^-$ (458.5) using O_2 as the collision gas and its reaction with O_2 instantly gave $[Fe_4S_4Cl_3O_2]^-$ (490.5) peak. Besides $[Fe_4S_4Cl_4]^{2-}$, $[Fe_4S_4Cl_3(SEt)]^{2-}$ is the only other species in the series $[[Fe_4S_4Cl_{4-x}(SEt)_x]^{2-}$ to produce O_2 substituted complex $[Fe_4S_4Cl_2(SEt)O_2]^-$. Interestingly, it was observed that this peak of O_2 substituted species appears together with the appearance of Cl^- and $[Fe_4S_4Cl_3]^-$ or $[Fe_4S_4Cl_2(SEt)]^-$, i.e., species with one empty iron site after the detachment of Cl^-.

Fig. 7 shows CID spectra of singly charged $[Fe_4S_4Cl_4]^-$. The obvious absence of the O_2 substitution channel indicates that direct interaction between O_2 and $[Fe_4S_4Cl_4]^-$ through an adduct intermediate, $[Fe_4S_4Cl_4O_2]^-$, to produce $[Fe_4S_4Cl_3O_2]^-$ can be excluded. In comparison to Fig. 2, the peak of $[Fe_4S_4Cl_3]^-$ was also absent from Fig. 7 indicating the absence of chlorine atom loss channel from singly charged precursor ion. This is understandable since Cl atom has high electron affinity it is hard to lose as a neutral atom.

Because formation of O_2 substituted species is always accompanied by Cl^- detachment and no O_2 substituted species is produced by CID of the singly charged $[Fe_4S_4Cl_4]^{1-}$ parent, we conclude that formation of dioxygen coordinated species involves a two-step mechanism. The first step is the detachment of one Cl^- caused by Coulomb repulsion Eq. (4). The empty iron site will be reactive enough to embrace a neutral O_2 molecule as a ligand Eq. (9)

$$[Fe_4S_4Cl_3]^- + O_2 \rightarrow [Fe_4S_4Cl_3O_2]^- \quad (9)$$

Interestingly, considering the electron affinity of O_2, after the attachment the O_2 molecule most possibly will attract more electron density from the cubane core and it is in fact more like an O_2^- coordination, similar to the transient intermediate proposed in the [4Fe-4S] cluster oxidation of aconitase and other Fe–S cluster containing hydrolyases [29]. In the biological environment, this O_2 molecule will eventually oxidize the cubane core, dragging one of the iron site off the cubane to form the Fe_3S_4 site and inactivate the protein [29]. Although the reaction condition in the gas phase is very different from that in solution, the observation that dioxygen can coordinate directly to this extremely air-sensitive [4Fe-4S] cubane structure without destroying it is surprising and has potential biological implication.

3.3. Neutral losses and hydrogen coordination in the CID products of –SEt containing cubanes

As discussed above, all the fragments from this series of doubly charged parents are singly charged species formed either by losing one electron or by splitting into two singly charged products. Since the singly charged species formed by electron detachment, $[Fe_4S_4Cl_{4-x}(SEt)_x]^-$, carry large amounts of internal energies, they are expected to undergo further fragmentation, giving rise to fragments observed in the *m/z* range between the parent dianions and the singly charged $[Fe_4S_4Cl_{4-x}(SEt)_x]^-$ anions. MS/MS spectra of all the parents containing more than one –SEt ligand exhibit two common features: loss of 62 u (HSEt) from $[Fe_4S_4Cl_{4-x}(SEt)_x]^-$, corresponding to the fragment formed by electron detachment from the precursor doubly charged anions, followed by loss of 60 u. Scheme 1 shows the mechanism proposed for this channel using $[Fe_4S_4(SEt)_4]^{2-}$ as an example.

The neutral loss of HSEt implies that there is a proton transfer from a nearby ligand –SEt, most possibly from the terminal methyl group, to the leaving ligand (Step 1). The structure of this fragment is interesting. Proton transfer results in formation of a negatively charged ligand $–SCH_2CH_2^-$ while loss of neutral HSEt produces an empty iron site. If the $–SCH_2CH_2^-$ chain were long enough, the negative charge end would combine with the empty iron site to form a ring structure. However, this chain with only two carbon atoms is too short for this conformation. Therefore, to avoid the unstable negatively charged $CH_2–$ group dangling outside the 4Fe-4S core with one empty iron site, $–SCH_2CH_2^-$ would rearrange to form a new ligand with a double bond, –SCH=CH_2, and generate one hydride ($–SCH_2CH_2^- \rightarrow –SCH=CH_2 + H^-$). This hydride will coordinate to the empty iron site instantly resulting in a stable product, such as $[Fe_4HS_4(SEt)_2(SCH=CH_2)]^-$ in the case of $x = 4$. This mechanism can also explain why we did not observe O_2 substituted products from the parents containing –SEt. With the hydrogen coordination there will be no more empty iron site for O_2 attachment. The fragmentation reaction for this step can be formulated for the series of parents as,

$$[Fe_4S_4Cl_{4-x}(SEt)_x]^- \rightarrow [Fe_4HS_4Cl_{4-x}(SEt)_{x-2}(SCH=CH_2)]^- + HSEt \quad (10)$$

where $x = 2$–4.

After the first neutral loss of HSEt (62 u), the subsequent loss of *m/z* 60 corresponds to neutral loss of HSCH=CH_2 (60 u), i.e., the combination of the newly formed ligand and the coordination hydrogen. The reactions are formulated as,

$$[Fe_4HS_4Cl_{4-x}(SEt)_{x-2}(SCH=CH_2)]^- \rightarrow [Fe_4S_4Cl_{4-x}(SEt)_{x-2}]^- + HSCH=CH_2 \quad (11)$$

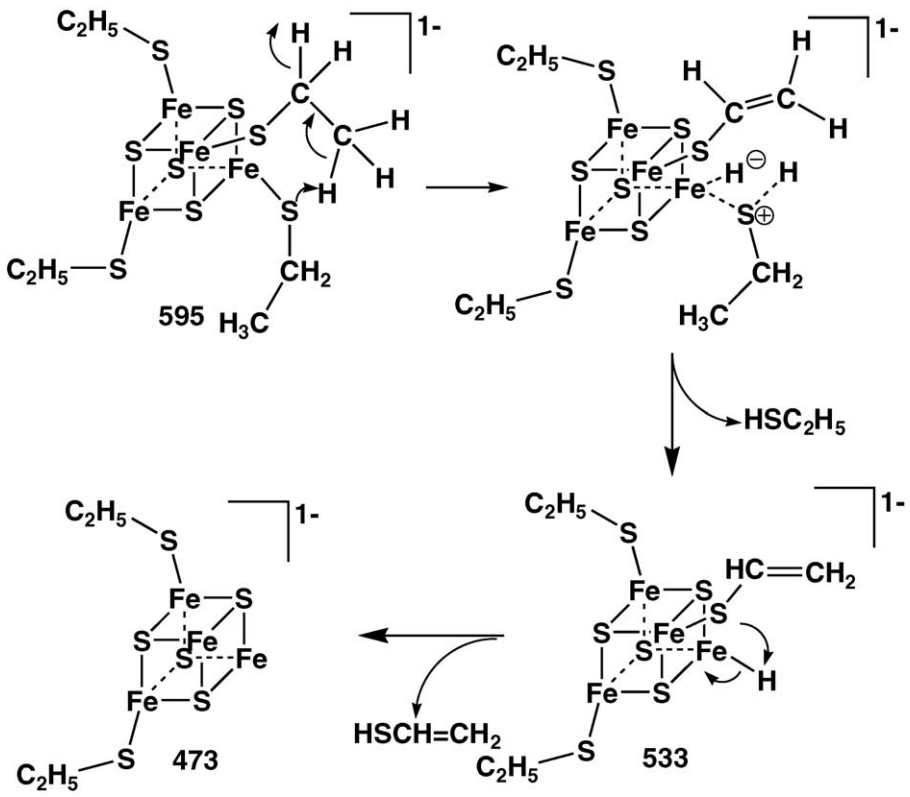

Scheme 1. Mechanism of the neutral molecular losses HSEt (62 u) and HSCH═CH_2 (60 u) from $[Fe_4S_4(SEt)_4]^-$ in the CID process.

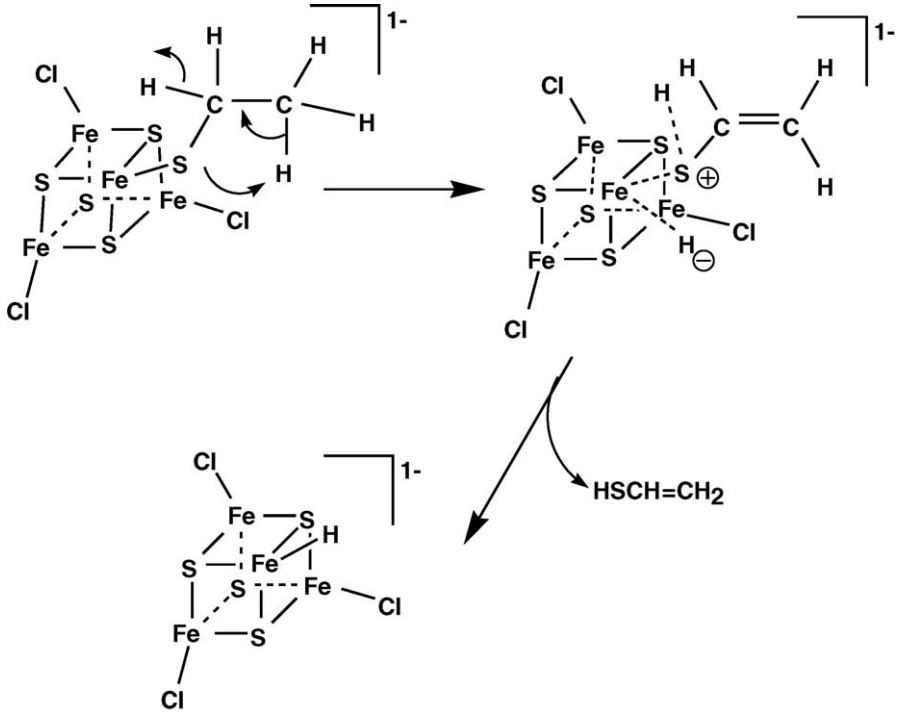

Scheme 2. Mechanism of the neutral molecular loss HSCH═CH_2 (60 u) from $[Fe_4S_4Cl_3(SEt)]^-$ in the CID process.

Furthermore, a 60 *m/z* loss, which can exclusively be assigned to $HSCH{=}CH_2$ (60 u), was observed from the parent $[Fe_4S_4Cl_3(SEt)]^-$ which contains only one SEt ligand. This provided additional evidence for the above mechanism. On the other hand, this $HSCH{=}CH_2$ loss from $[Fe_4S_4Cl_3(SEt)]^-$ implies an intra-ligand proton transfer ($-SC_2H_5 \rightarrow HSCH{=}CH_2 + H^-$) generating a hydride which would coordinate to the empty iron site to satisfy the iron coordination requirement,

$$[Fe_4S_4Cl_3(SEt)]^- \rightarrow [Fe_4HS_4Cl_3]^- + HSCH{=}CH_2 \quad (12)$$

The mechanism for this reaction is proposed in Scheme 2.

Interestingly, a similar 60 u loss was also observed from the singly charged species $[Fe_4S_4Cl_2(SEt)]^-$ (482.6) formed from $[Fe_4S_4Cl_3(SEt)]^-$ (517.6) after Cl^- detachment.

$$[Fe_4S_4Cl_2(SEt)]^- \rightarrow [Fe_4HS_4Cl_2]^- + HSCH{=}CH_2 \quad (13)$$

SORI CID experiment on $[Fe_4S_4(SEt)_4]^{1-}$ (595.7) generated in the source (Fig. 8) provides further support of the proposed mechanism of neutral loss that involves electron detachment from the doubly charged precursor ion in the first step. Specifically, the same neutral losses of HSEt (62 u) and $HSCH{=}CH_2$ (60 u) give two peaks at 533.7 and 473.7, corresponding to the respective neutral losses from high collision energy fragmentation of $[Fe_4S_4(SEt)_4]^{2-}$ (298.3). The mass peaks in the low mass range of Fig. 8 were assigned to reaction products of O_2 with the cubane fragments using accurate mass assignment.

Fig. 9 shows the results of SID experiments carried out on $[Fe_4S_4(SEt)_4]^-$. The spectrum shows the same two neutral losses of 62 u and 60 u as the CID results, but it is much cleaner in the low mass range (<383) without the oxygen related peaks (Fig. 8). A new species $[Fe_4S_4(SEt)S]^-$ appeared at $m/z = 444$ representing a radical loss of $^{\bullet}C_2H_5$ from $[Fe_4S_4(SEt)_2]^-$ instead of 445 $[Fe_4S_4(SEt)(SH)]^-$, a neutral loss of $CH_2{=}CH_2$ (Fig. 8).

The observation of hydride-coordinated iron site in the cubane complexes is quite interesting. The proposed mechanism showed a sequence of proton migration, neutral ligand loss (HSEt), and hydrogen coordination. This process is surprisingly similar to the one proposed for proton reduction by $[Fe_4S_4(SPh)_4]^{3-}$ in the solution kinetic studies [30–32]. In the proposed mechanism, the first step is the tri-protontation to form $[Fe_4S_2(SH)_2(HSPh)(SPh)_3]$, followed by dissociation of the neutral HSPh with a empty iron site to form $[Fe_4S_2(SH)_2(SPh)_3]$, and finally protonation of the empty iron site to form $[Fe_4HS_2(SH)_2(SPh)_3]^+$. It should be noted that the most important intermediate $[Fe_4HS_2(SH)_2(SPh)_3]^+$ in this mechanism, despite its two protonated bridging sulfur ligands, has the same oxidation state and similar structure proposed for the species we observed in our CID and SID experiments in the gas phase. The formation of hydrogen coordination to iron site in Fe–S proteins have been proposed as catalytic intermediates in both the hydrogenases [33–35] and nitrogenases [36–38].

4. Conclusions

CID experiments of a series of doubly charged 4Fe-4S cluster ion $[Fe_4S_4Cl_{4-x}(SEt)_x]^{2-}$ ($x = 0$–4) exhibited several very interesting fragmentation channels and products. Although the electron detachment, Cl^- detachment, and symmetric fission of the cubane core are all related to the doubly charged nature of the parents, they exhibit different behavior with the change of coordination environment. The significance of the electron detachment increases with decreasing electron binding energies, while the efficiency of both the symmetric fission of the cubane core and Cl^- detachment increases with increasing Coulomb repulsion. In spite of the asymmetric terminal ligand coordination, the fission of the cubane core occurred for the mixed ligand parents, demonstrating the robustness of the two layer structure. Neutral losses from −SEt containing parent generated hydrogen coordinated [4Fe-4S] clusters via inter- or intra-ligand proton migration, a mechanism similar to that proposed for proton reduction by $[Fe_4S_4]^+$ complex. O_2 substituted products became increasingly significant with increasing coulomb repulsion in the doubly charged parents. It was proposed that the O_2 attachment could only occur after the dissociation of one Cl^-. These unique observations may have important implications both chemically and biologically and deserve further experimental and theoretical investigations.

Acknowledgments

This work was supported by the National Institutes of Health (GM-63555 to L.S.W.) and the Chemical Science Division of the Office of Basic Energy Sciences, U.S. Department of Energy (to J.L.). The experimental work was performed at the W. R. Wiley Environmental Molecular Sciences Laboratory, a national scientific user facility sponsored by DOE's Office of Biological and Environmental Research and located at Pacific Northwest National Laboratory, which is operated for DOE by Battelle.

References

[1] W. Lovenberg (Ed.), Iron–Sulfur Proteins, vol. I and II, Academic Press, New York, 1973.
[2] T.G. Spiro (Ed.), Iron–Sulfur Proteins, Wiley-Interscience, New York, 1982.
[3] R. Cammack, Adv. Inorg. Chem. 38 (1993) 281.
[4] H. Beinert, R.H. Holm, E. Munck, Science 277 (1997) 653.
[5] X.B. Wang, S. Niu, X. Yang, S.K. Ibrahim, C.J. Pickett, T. Ichiye, L.S. Wang, J. Am. Chem. Soc. 125 (2003) 14072.
[6] Y.J. Fu, X. Yang, X.B. Wang, L.S. Wang, Inorg. Chem. 43 (2004) 3647.
[7] X. Yang, S. Niu, T. Ichiye, L.S. Wang, J. Am. Chem. Soc. 126 (2004) 15790.
[8] X. Yang, X.B. Wang, Y.J. Fu, L.S. Wang, J. Phys. Chem. A 107 (2003) 1703.
[9] X. Yang, X.B. Wang, S.Q. Niu, C.J. Pickett, T. Ichiye, L.S. Wang, Phys. Rev. Lett. 89 (2002) 163401.
[10] X. Yang, X.-B. Wang, L.-S. Wang, Int. J. Mass Spectrom. 228 (2003) 797.
[11] S. Niu, X.-B. Wang, X. Yang, L.-S. Wang, T. Ichiye, J. Phys. Chem. A 108 (2004) 6750.
[12] L. Noodleman, E.J. Baerends, J. Am. Chem. Soc. 106 (1984) 2316.
[13] L. Noodleman, D.A. Case, Adv. Inorg. Chem. 38 (1992) 423.

[14] L. Noodleman, C.Y. Peng, D.A. Case, J.M. Mouesca, Coord. Chem. Rev. 144 (1995) 199.
[15] Y.-J. Fu, X. Yang, X.-B. Wang, L.-S. Wang, J. Phys. Chem. A 109 (2005) 1815.
[16] Y.-J. Fu, S.-Q. Niu, T. Ichiye, L.-S. Wang, Inorg. Chem. 44 (2005) 1202.
[17] H.-J. Zhai, X. Yang, Y.-J. Fu, X.-B. Wang, L.-S. Wang, J. Am. Chem. Soc. 126 (2004) 8413.
[18] J. Laskin, E.V. Denisov, A.K. Shukla, S.E. Barlow, J.H. Futrell, Anal. Chem. 74 (2002) 3255.
[19] L.J. de Koning, N.M.M. Nibbering, S.L. van Orden, F.H. Laukien, Int. J. Mass Spectrom. Ion Process. 165/166 (1997) 209.
[20] G. Kruppa, P.D. Schnier, K. Tabei, S.L. van Orden, M.M. Siegel, Anal. Chem. 74 (2002) 3877.
[21] J.W. Gauthier, T.R. Trautman, D.B. Jacobson, Anal. Chim. Acta 246 (1991) 211.
[23] J. Laskin, J. Futrell, Mass Spectrom. Rev. 22 (2003) 158.
[24] J. Laskin, E. Denisov, J.H. Futrell, J. Am. Chem. Soc. 122 (2000) 9703.
[25] J. Laskin, M. Byrd, J. Futrell, Int. J. Mass Spectrom. 195/196 (2000) 285.
[26] L.-S. Wang, C.F. Ding, X.B. Wang, J.B. Nicholas, Phys. Rev. Lett. 81 (1998) 2667.
[27] X.-B. Wang, J.B. Nicholas, L.-S. Wang, J. Chem. Phys. 113 (2000) 653.
[28] X.-B. Wang, L.-S. Wang, Nature 400 (1999) 245.
[29] D.H. Flint, R.M. Allen, Chem. Rev. 96 (1996) 2315.
[30] K.L.C. Gronberg, R.A. Henderson, K.E. Oglieve, Dalton (1998) 3093.
[31] A.J. Dunford, R.A. Henderson, Inorg. Chem. 41 (2002) 5487.
[32] A.J. Dunford, R.A. Henderson, Chem. Commun. (2002) 360.
[33] D.S. Homer, B. Heil, T. Happe, T.M. Embley, Trends Biochem. Sci. 27 (2002) 148.
[34] X. Zhao, C.Y. Chiang, M.L. Miller, M.V. Rampersad, M.Y. Darensbourg, J. Am. Chem. Soc. 125 (2002) 518.
[35] T. Zhou, Y. Mo, A. Liu, K.R. Tsai, Inorg. Chem. 43 (2004) 923.
[36] J. Liang, R.H. Burris, Proc. Natl. Acad. Sci. U.S.A. 85 (1988) 9446.
[37] M.C. Durrant, Biochem. J. 355 (2001) 569.
[38] M.C. Durrant, Biochemistry 41 (2002) 13946.